REPORT DOCUMENTATION PAGE

AFRL-SR-AR-TR-05-

0127

1. REPORT DATE *(DD-MM-YYYY)*	2. REPORT TYPE	3. DATES COVERED *(From - To)*
30-3-2005	Final	Jan. 1-2002-Dec. 31, 2004

4. TITLE AND SUBTITLE
Relativistic Magnetron Priming Experiments and Theory

5a. CONTRACT NUMBER

5b. GRANT NUMBER
F49620-02-1-0089

5c. PROGRAM ELEMENT NUMBER

6. AUTHOR(S)
R.M. Gilgenbach and Y.Y. Lau

5d. PROJECT NUMBER

5e. TASK NUMBER

5f. WORK UNIT NUMBER

7. PERFORMING ORGANIZATION NAME(S) AND ADDRESS(ES)
University of Michigan
Ann Arbor, MI 48109

8. PERFORMING ORGANIZATION REPORT NUMBER

9. SPONSORING/MONITORING AGENCY NAME(S) AND ADDRESS(ES)
Air Force Office of Scientific Research
4015 Wilson Blvd.
Arlington, VA 22203

NE

10. SPONSOR/MONITOR'S ACRONYM(S)
AFOSR

11. SPONSOR/MONITOR'S REPORT NUMBER(S)

12. DISTRIBUTION/AVAILABILITY STATEMENT
Unlimited

DISTRIBUTION STATEMENT A
Approved for Public Release
Distribution Unlimited

13. SUPPLEMENTARY NOTES
none

14. ABSTRACT

Microwave/ RF priming experiments have been performed on the UM relativistic magnetron. The high power RF priming source (40 kV, non-relativistic magnetron) was obtained on-loan from the Air Force Research Lab. Microwave power output from the AFRL priming magnetron was input into one arm of the three-waveguide extraction system on the relativistic magnetron. The UM/ Titan A6 relativistic magnetron was driven by MELBA-C; the ceramic insulator yields 10-8 Torr scale vacuum for quasi-hard-tube conditions. Microwave priming experiments showed mode-beating effects at power levels and frequency detuning consistent with Adler's equation. Effects of microwave priming on start-oscillation time and microwave pulselength were also characterized. Major breakthroughs in this research were the discovery and demonstration of two new magnetron priming techniques: magnetic priming and cathode priming. Magnetic priming was patented by UM (US patent No. 6,872,929).

15. SUBJECT TERMS
magnetron, high power microwaves, magnetron-priming, cathodes

16. SECURITY CLASSIFICATION OF:			17. LIMITATION OF ABSTRACT	18. NUMBER OF PAGES	19a. NAME OF RESPONSIBLE PERSON
a. REPORT	b. ABSTRACT	c. THIS PAGE			Ronald M. Gilgenbach
U	U	U	UU	35	19b. TELEPHONE NUMBER *(Include area code)* 734-763-1261

FINAL TECHNICAL REPORT TO:

Dr. ROBERT J. BARKER
THE AIR FORCE OFFICE OF SCIENTIFIC RESEARCH

FOR THE PROJECT:

RELATIVISTIC MAGNETRON PRIMING EXPERIMENTS AND THEORY

AFOSR GRANT NUMBER: F49620-02-1-0089

SUBMITTED BY:

RONALD M. GILGENBACH, PROFESSOR and
Y.Y. LAU, PROFESSOR
INTENSE ENERGY BEAM INTERACTION LAB
NUCLEAR ENGINEERING AND RADIOLOGICAL SCIENCES DEPARTMENT
UNIVERSITY OF MICHIGAN
ANN ARBOR, MI 48109-2104

MARCH 2005

RELATIVISTIC MAGNETRON PRIMING EXPERIMENTS AND THEORY
AFOSR GRANT NUMBER: F F49620-02-1-0089

TABLE OF CONTENTS

1.0 EXECUTIVE SUMMARY

Microwave/ RF priming experiments have been performed on the UM relativistic magnetron. The high power RF priming source (40 kV, non-relativistic magnetron) was obtained on-loan from the Air Force Research Lab. Microwave power output from the AFRL priming magnetron was input into one arm of the three-waveguide extraction system on the relativistic magnetron. The UM/Titan A6 relativistic magnetron was driven by MELBA-C; the ceramic insulator yields 10^{-8} Torr scale vacuum for quasi-hard-tube conditions.

Microwave priming experiments showed mode-beating effects at power levels and frequency detuning consistent with Adler's equation. Effects of microwave priming on start-oscillation time and microwave pulselength were also characterized.

Major breakthroughs in this research were the discovery and demonstration of two new magnetron priming techniques: *magnetic priming and cathode priming.* Magnetic priming was patented by UM (US patent No. 6,872,929): Low-Noise Crossed Field Devices Such as a Microwave Magnetron, Microwave Oven Utilizing Same and a Method of Converting a Noisy Magnetron to a Low-Noise Magnetron, issued March 29, 2005. In this concept, N/2 azimuthal magnetic perturbations are applied to an N-cavity magnetron. The effectiveness of magnetic priming is due to prebunching of the electrons near the cathode surface, and to a newly discovered parametric instability which brings electrons to the anode before the excitation of any RF mode. Noise reduction and startup enhancement have been demonstrated in kW magnetrons. MAGIC Code simulations of magnetic priming have shown rapid startup in relativistic magnetrons.

In the second, new technique, cathode priming, the three electron spokes desired for pi-mode (in an A6 magnetron) are generated by creating three azimuthal emission zones on a cathode. The advantages of cathode priming are: a) faster start-oscillation, b) mode-locking into the desired pi mode; these advantages have been demonstrated in experiments and verified in 2-D and 3D MAGIC Code simulations.

Another invention, projection-ablation lithography (PAL) provided a new technique for fabricating monolithic, metal cathodes. These all metal, PAL cathodes have shown advantages, including:

1) High-current densities,
1) emission regions micro-machined by a laser to provide desired level of field enhancement,
1) emission regions heat-sinked to base cathode,

1) no outgassing for all-metal construction,
1) little or no plasma closure, and
1) cathode priming easily implemented.

Close collaborations have been maintained with scientists from the Air Force Research Laboratory. AFRL provided the MW level priming magnetron and power modulator, as well as pulsed electromagnets on loan to UM. AFRL 3-D ICEPIC simulations also guided UM experiments.

Executive Summary of Students and Personnel Involvement in This research

Faculty:

Prof. R.M. Gilgenbach
Prof. Y.Y Lau

Graduate Students:

1) Mike Lopez: Ph.D. dissertation title: "Experiments on a Relativistic Magnetron driven by a Microsecond Electron Beam Accelerator with a Ceramic Insulating Stack" defended in 2003, employed by Sandia National Lab

2) Michael Jones: PhD dissertation title: "Cathode Priming of a Relativistic Magnetron using Multi-Emission Zones on Projection Ablation Lithography Cathodes". Defense on April 11, 2005. Will be employed by Sandia National Labs

3) V. Bogdan Neculaes: Ph.D. Dissertation Title: Magnetron Magnetic priming for Rapid Startup and Noise Reduction". Defense on April 11, 2005. Will be employed by GE Research Labs

4) W. White, Ph.D. candidate, expected PhD dissertation title: "Radio-Frequency Priming of a Long-Pulse, Relativistic Magnetron" degree expected in 2006

Undergraduate Students

1) Matt Gomez, will attend graduate school
1) Jacob Zier, will attend graduate school

2.0 EXPERIMENTAL CONFIGURATION

2.1 MELBA Accelerator and Magnetron

The experimental configuration is depicted schematically in Figure 1 and pictorially in Figure 2. There are two magnetrons in these experiments. The priming magnetron, obtained on-loan from AFRL, is a 40 kV, non-relativistic magnetron, driven by a hard-tube modulator. The relativistic magnetron, shown in Fig. 3, is a 6-vane type on loan from Titan Corporation, Pulse-Sciences Division (Dr. David Price). This magnetron typically operated at -300kV, 5-10 kA, 0.3-0.5 μs, with the pi mode at 1.03 GHz. However, the priming source frequency is 1.27-1.3 GHz. This necessitated fabrication and installation of tuning stubs (Fig. 3) into the cavities to raise the relativistic magnetron's natural frequency to match that of the priming magnetron. AFRL simulations and later UM experiments verified that the pi-mode was favored by the three-fold symmetry of a three-waveguide extraction system, which was utilized for most experiments. [7] Two of the three-extraction waveguides are terminated in UM-built water loads and power is monitored by calibrated (-60 dB) coupling loops in one arm. The third (priming) waveguide is attached through a UM-built TR switch and ferrite isolator to the AFRL priming magnetron output. Signals are transmitted by coaxial cable to the Faraday cage where they are diagnosed for power and spectrum by time-frequency-analysis (TFA). MELBA's ceramic insulator stack permits base vacuum of 8.5×10^{-8} Torr, near hard-tube conditions. The MELBA cathode extends out of the vacuum chamber and into the magnetron by a 1.27cm diameter aluminum rod that acts as the cathode stalk.

Projection ablation lithography cathodes were tested and utilized on MELBA for comparison with the previous fabric cathodes.[5] The

experimental configuration for excimer laser Projection-Ablation-Lithography (PAL) cathodes is depicted in Figure 4. Field emission patterns are etched into the metal cathode by laser ablation of a demagnified projection on a metal screen. The resulting patterns have structures with dimensions of some hundred-microns , as depicted in the scanning electron microscope (SEM) photos in Figure 5. When ablated in air, small particulate matter was also redeposited on the cathode, which might aid in field emission of electrons.

Another innovation at UM was the invention of cathode priming, in which N/2 azimuthal emission regions are etched in the cathode for an N-cavity magnetron.[4,5] The three emission zones generate the 3 electron spokes required for pi-mode oscillation of the 6-cavity magnetron. The configuration of a three-emission zone cathode is depicted in Fig. 6 for the A6 magnetron, denoted Tri-PAL. Five PAL cathodes were tested on MELBA; three with uniform emission zones and two with cathode priming.

3.0 Summary of Experimental Results

This section summarizes the major experimental findings of this research project. More detailed waveforms are found in the three annual technical reports already submitted.

Figure 7 depicts time-frequency-analysis (TFA) data for two shots in which microwave priming signals (~300 kW) were injected at 1.28 GHz, close to the 2*pi/3 mode for the relativistic magnetron with tuning stubs. Data is in the upper TFA shows that the magnetron begins oscillation

close to the priming frequency, but eventually slips back into the lower natural frequency of the relativistic magnetron. The lower data set demonstrates that the relativistic magnetron initially starts oscillation at the priming frequency and maintains this frequency during the entire high power oscillation.

Time-frequency-analysis data in Fig. 8 clearly show the phenomenon of mode-beating between the priming magnetron and the relativistic magnetron. Analysis of these data yields a beating-time of about 10 ns. This experimentally measured time agrees well with the theoretically predicted beating time of 11 ns, obtained from the difference frequency between the two magnetrons.

Experimental data are in agreement with Adler's equation, which relates the required priming power to the frequency detune between the sources. This topic is discussed further in the theory section of this report.

Experiments were performed on the relativistic magnetron to test the concept of cathode priming.[4,5] The Tri-PAL cathode was utilized for these experiments. Results of these experiments are summarized in Figure 9, which compares the microwave start-oscillation time for the Tri-PAL cathode (cathode priming) to previous cotton cathode and single emission zone cathodes (PAL-I and PAL-II). Clearly, the cathode priming case exhibits the fastest start-oscillation time. Furthermore, all PAL cathodes tested showed more rapid start-oscillation than the cotton cathode.

For long-pulse microwave generation an important figure of merit for cathodes is the plasma closure velocity; (lower is better). Summary data in Figure 10 indicates that all-metal PAL cathodes demonstrate much slower closure velocity than previous cotton cathodes. The standard deviation bars on the plot also show that in some cases, plasma closure velocity was close to zero for PAL cathodes.

Microwave oscillation time, summarized in Figure 11, shows that all three PAL cathodes generated longer microwave pulses than the cotton cathode in the relativistic magnetron. The longest microwave pulselength was exhibited by the PAL-II cathode, which generated the highest current, but also the highest closure velocity. The Tri-PAL cathode pulselength was similar to the PAL-I cathode.

A significant measure of a cathode's success is the electronic efficiency of microwave generation in the relativistic magnetron, summarized in Figure 12. Clearly, the Tri-PAL cathode (cathode priming) exhibits the highest electronic efficiency (some 17%). This effect is believed due to the rapid prebunching of the electrons into the desired three-spoke structure required for pi-mode microwave oscillation.

4.0 MAGIC Code Simulations of Cathode Priming

Extensive computational simulations of cathode priming were performed utilizing the MAGIC code in two and three dimensions.[4,5] Figure 13 depicts results of preliminary 2-D MAGIC Code simulations of cathode

priming in an A6 magnetron with similar parameters to the UM-Titan tube. These simulations show the RF electric field for three cases:

1) single emission zone (without cathode priming),
2) cathode priming with the cathode placed under the cavities (low electric field region), and
3) cathode priming with emission zone placed under the vanes (high electric field region).

These data clearly demonstrate the advantages of cathode priming, both cases of which show much faster start-oscillation than the unprimed case. The cathode priming case of emission regions under the vanes shows even faster (up to factor of 3) startup than the unprimed case, apparently because the higher electric field yields higher current density.

Results of 3-D MAGIC Code simulations are shown in Figure 14, comparing cathode priming to the uniform emission zone. At a simulation time of 6.5 ns, the cathode priming case clearly forms three electron spokes required for pi-mode oscillation. By contrast at the same simulation time, the unprimed case shows the smooth Brillouin hub, with no evidence of spoke formation.

The instantaneous frequency is a measure of the mode purity (or competition) of the relativistic magnetron. Figure 15 presents 3-D MAGIC simulation data of instantaneous frequency for the same 3 cases as figure 13 (in 2D). Both cathode priming cases start-oscillation immediately in the pi mode and remain locked into this desired mode. However, it is apparent that the unprimed case, the magnetron oscillates first in the undesired 2*pi/3 mode, encounters mode competition and finally after

some 30 ns begins to oscillate in the pi-mode. These data confirm that cathode priming can mode-lock relativistic magnetrons into the desired pi-mode.

5.0 Theoretical Results

The recent success of magnetic priming of the kW oven magnetron [1-3, 6, 8, 9, 11] created a profound impact on the thinking of relativistic magnetron priming. Three types of priming processes can now be envisioned,

1. Magnetic priming
2. Cathode priming
3. RF priming

instead of just Item 3, RF priming, as originally proposed. In fact, the first two hold considerable promise over the third, especially for relativistic magnetrons. In this Final Report, we shall address the theoretical progress on all three.

1. Magnetic priming

By the use of a periodic azimuthal perturbation on the axial magnetic field, the start-up of the pi-mode is substantially hastened.[9, 11] By first studying the nonrelativistic, thermionic magnetron, we discover a parametric instability in the electron orbits which provide instantaneous creation of the electron spokes, even before the rf mode is excited.[12]

This is a very important discovery, because even in the MAGIC simulations, startup is a major issue.

The fact that there is an orbital instability can be appreciated because there is a parametric resonance condition involving the three intrinsic frequencies in magnetic priming,

$$\Omega_1 - \Omega_2 = m\Omega_3, \quad m = 1, 2, 3, 4, .. \qquad (1)$$

where Ω_1 and Ω_2 are respectively the maximum and minimum cyclotron frequencies in magnetic priming, and Ω_3 is inversely proportional to the transit time of an electron through one magnetic perturbation period. When Eq. (1) is satisfied, electrons are drawn to the cathode even before the rf mode is excited. Thus startup is hastened.

Equation (1) is satisfied only over certain bands of magnetic field perturbation strength. Figure 16 shows these bands of $\alpha = (\Omega_1 - \Omega_2)/\Omega_1$, which measures the magnetic priming strength. ICEPIC simulation of the thermionic oven magnetron (by Luginsland [6]) strongly suggests the presence of this orbital instability when magnetic priming is included.

However, it is not clear if the orbital parametric instability is operative in a relativistic magnetron. The latter is almost always in the space charge limited regime, in which the electron orbits are rather different. Recent MAGIC simulations of the A6 magnetron does show that magnetic priming is in fact effective over certain bands of α [Fig. 17]. That is, the start-up time of the pi-mode is substantially reduced for certain values of α. But

whether this is related to the orbital parametric instability remains to be examined.

2. Cathode Priming

Cathode priming is a very promising approach for relativistic magnetrons.[4,5] The concept is so new that we have not had any substantive theory on this topic. The experimental data on cathode priming collected to date raise the following issues (for future investigations):

a. Where, and how, are the electrons emitted in the PAL cathode?
b. While the startup for the pi-mode is hastened, why is the microwave pulselength still short?
c. How important is the tangential electric field on the PAL cathode surface in the initiation of the spokes?
d. What is the proper theoretical model for cathode priming?
e. In the 3K configuration (the cathode consists of 3 separate rods instead of the PAL cathodes described in previous sections), what is meant by a Brillouin hub? What is the effect of the rather significant azimuthal RF electric field between the rods? How about the non-removal of those unfavorable electrons which may now hang around the interaction space (they are not removed because the cathode is not one solid piece in the 3K configuration)? Is there the advantage of enhanced current density for the 3K configuration, because of the 2D effects of the Child-Langmuir law?

3. RF priming

We have found that the RF priming experiment on the relativistic magnetron reported above is consistent with the Adler condition. We have also successfully interpreted the beating phenomenon observed in the time-frequency analysis in terms of the interference between the injected signal and the free running pi-mode.

The above phenomena have been subjected to a more refined study using the oven magnetron. This study, about to be written up for publication, compares Adler's mode locking theory against the RF priming experiments. The preliminary results are shown in Figs. 18 and 19. Figures 18 (top) and 19 (top) show the theoretical model of the power output of the driven oscillator, in which the free-running frequency of the (zero drive) oscillator is unity and the external drive has a scaled amplitude E_1 and variable frequency. Figures 18 (bottom) and 19 (bottom) show the experimental data at different drive powers and frequencies, with the free running magnetron oscillator at a frequency of 2.4511 GHz and output power of 825W. The qualitative agreement between theory and experiment is remarkable, given the simplicity of the theory and the complexity of a magnetron.

6.0 Collaborations with Air Force Research Lab Scientists

Extensive collaborations have been undertaken between University of Michigan faculty/ students and scientists at the Air Force Research Lab, Kirtland AFB, NM. Crucial, major equipment was loaned to UM by AFRL: pulsed electromagnets and microwave priming modulator/ magnetron. A book chapter was coauthored by UM faculty and AFRL scientists Tom Spencer and Keith Cartwright. Tom Spencer also served as a member on 3 UM student doctoral committees and coauthored many refereed publications with UM students and faculty. AFRL 3-D ICEPIC simulations have provided excellent guidance for UM experimental research.

7.0 US Patent Resulting from this Research

US patent (No. 6,872,929): Low-Noise Crossed Field Devices Such as a Microwave Magnetron, Microwave Oven Utilizing Same and a Method of Converting a Noisy Magnetron to a Low-Noise Magnetron, issued March 29, 2005

8.0 References: Refereed Journal Publications From This Research

1) V.B Neculaes, M.C. Jones, R.M. Gilgenbach, Y.Y Lau, J.W. Luginsland, W. White, N.M. Jordan, P. Pengvanich, Y. Hidaka and H. Bosman, "Magnetic Priming Effects on Noise, Startup and Mode Competition in Magnetrons", IEEE Transactions on Plasma Science, Special Issue of Invited Papers from ICOPS 2004, published in 2005

2) V.B. Neculaes, M.C, Jones, R.M. Gilgenbach, Y.Y. Lau, J.W. Luginsland, W.M. White, N.M. Jordon, P.Pengvanich, Y. Hidaka, "Magnetic Perturbation effects on Noise and Starup in DC Operating Oven Magnetrons", IEEE Transactions on Electron Devices, Special Issue of IVEC papers, 2005

3) M.C. Jones, V.B. Neculaes, W.M. White, Y.Y. Lau, R.M. Gilgenbach, J.W. Luginsland, P. Pengvanich, N.M. Jordan, Y. Hidaka, and H.L. Bosman, "Simulations of Magnetic Priming in a Relativistic Magnetron", submitted to IEEE Transactions on Electron Devices, Special Issue of IVEC papers, 2005

4) M.C. Jones, V.B. Neculaes, Y.Y. Lau, R.M. Gilgenbach, and W. M. White, Cathode Priming of a relativistic Magnetron", Applied Physics Letters, Vol. 85, p6332, Dec. 27, 2004

5) M.C. Jones, V.B. Neculaes, R.M. Gilgenbach, W.M. White, M.R. Lopez, Y.Y. Lau, T.A. Spencer, and D. Price, "Projection Ablation Lithography Cathode for High Current Relativistic Magnetron", Review of Scientific Instruments, Vol. 75, p 2976, Sept. 2004

6) Luginsland, Lau, Neculaes, Frese, Watrous, Gilgenbach and Jones, "Three-Dimensional Particle in Cell Simulations of Rapid-Startup in Strapped Oven magnetrons Due to Variation in the Insulating magnetic Field", Applied Physics Letters, 84 5425 (2004)

7) Mike R. Lopez, Ronald M. Gilgenbach, Michael C. Jones,
William M. White, David W. Jordan, Mark. D. Johnston, Trevor S. Strickler, V. Bogdan Neculaes, Y. Y. Lau, Thomas A. Spencer, Michael D. Haworth, Keith L. Cartwright, Peter J. Mardahl, John W. Luginsland, and David Price, "Relativistic Magnetron Driven by a Microsecond E-Beam Accelerator with

a Ceramic Insulator", IEEE Transactions on Plasma Science, Special Issue on High Power Microwaves, 32, 1171, (June 2004)

8) V.B. Neculaes, R.M. Gilgenbach, Y.Y. Lau, M.C. Jones, and W. White, Low-noise microwave oven magnetrons with fast start-oscillation by azimuthally varying axial magnetic fields", IEEE Transactions on Plasma Science, Special Issue on High Power Microwaves, 32, 1152, (June 2004)

9) M.C. Jones, V.B. Neculaes, W. White, Y.Y. Lau, and R.M. Gilgenbach, "Simulation of rapid startup in microwave magnetrons with azimuthally varying axial magnetic fields", Applied Physics Letters, 84, p1016, (2004).

10) "Limiting Current in a Relativistic Diode Under the Condition of Magnetic Insulation", M. Lopez, Y.Y. Lau, R.M. Gilgenbach, D.W. Jordan, J.W. Luginsland, Physics of Plasmas, 10, 4489, (2003)

11) "Low-noise microwave magnetrons by azimuthally varying axial magnetic field", V.B. Neculaes, R.M. Gilgenbach, and Y.Y. Lau, Applied Physics Letters, 83, p1938 (2003).

12). V. B. Neculaes, P. Pengvanich, Y. Hidaka, Y. Y. Lau, R. M. Gilgenbach, W. White, M. C. Jones, H. Bosman, and J. W. Luginsland, "Rapid Kinematic Bunching and Parametric Instability in a Crossed-Field Gap with a Periodic Magnetic Field," (in press, IEEE Trans. Plasma Sci., 2005).

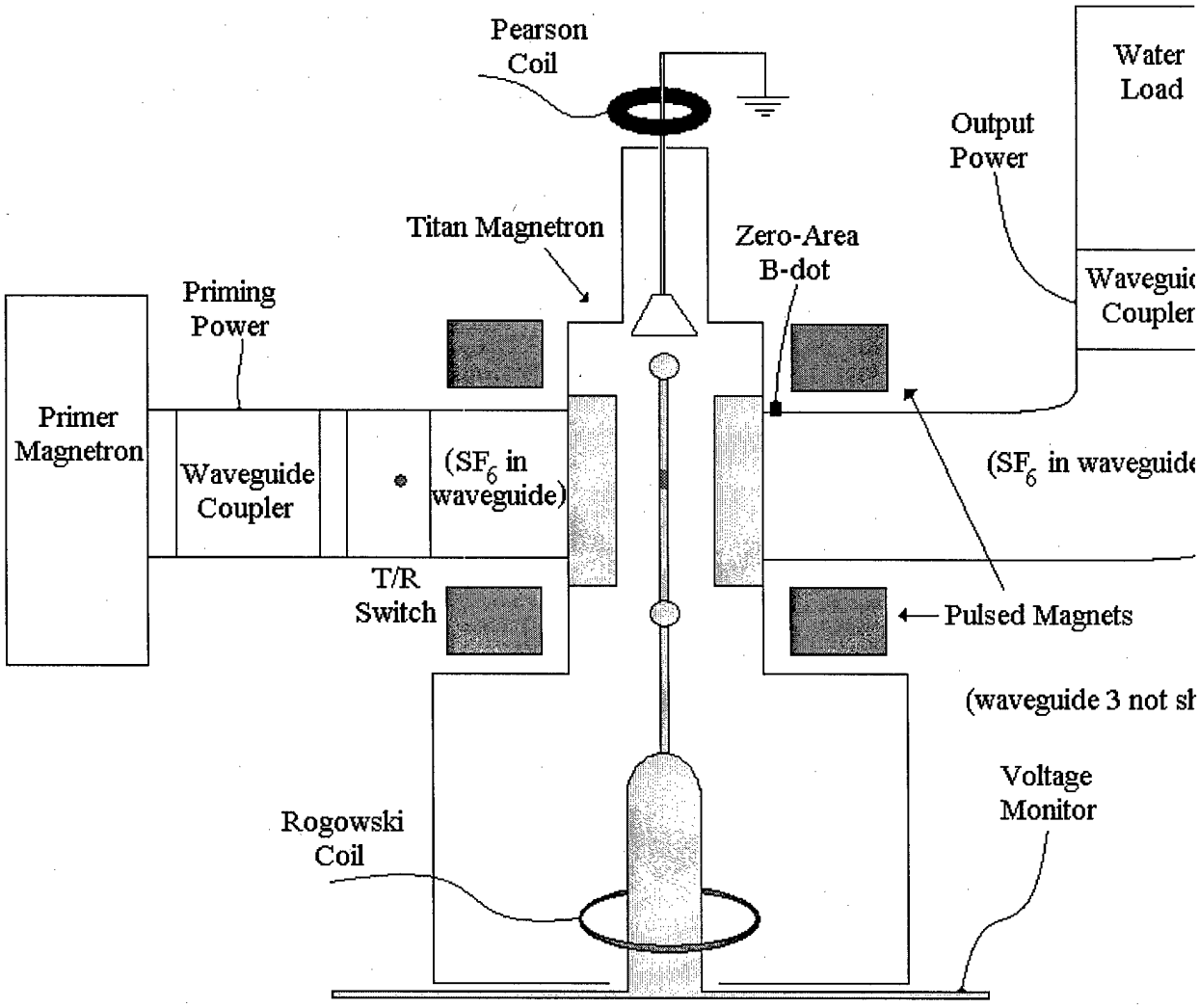

Figure 1: Michigan Relativistic Magnetron Facility Diagram (RF Priming).

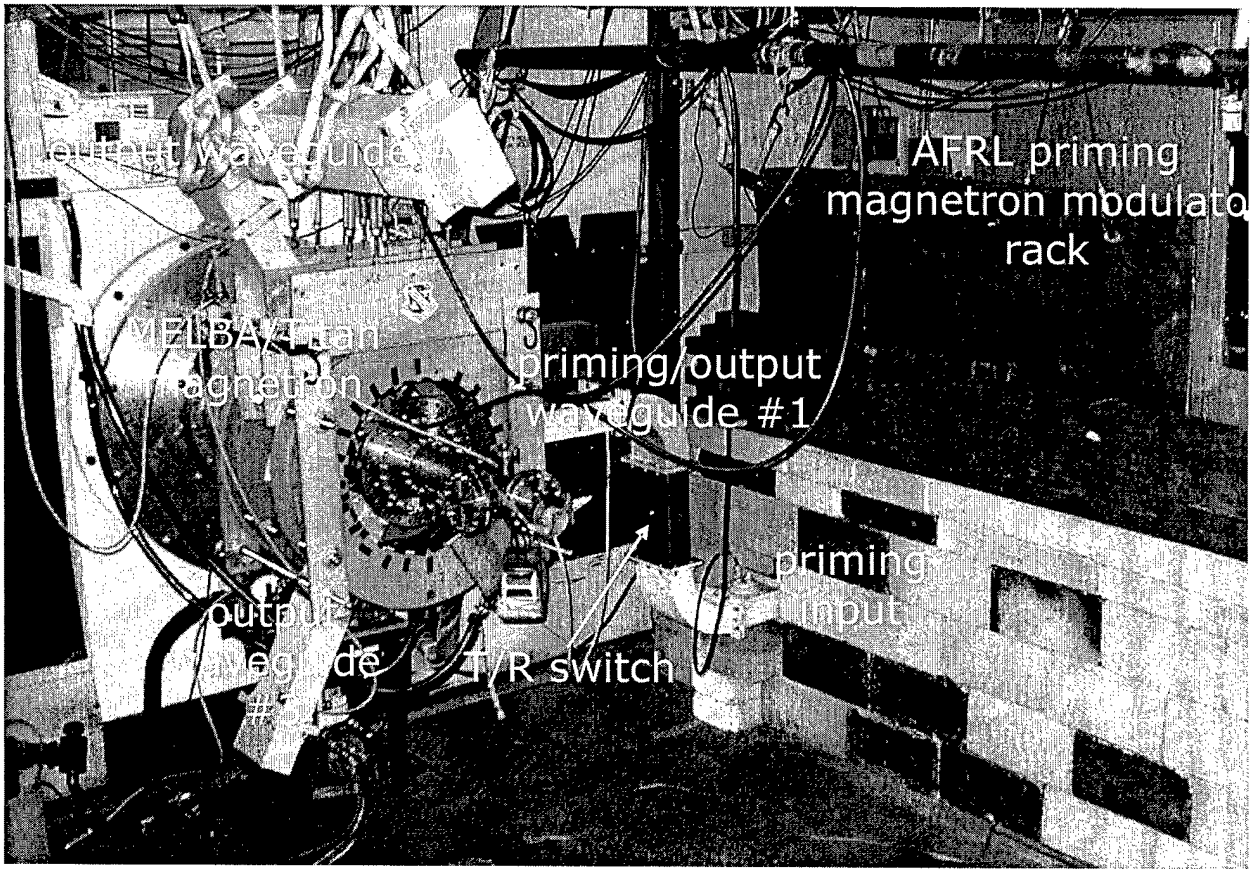

Figure 2: Michigan Relativistic Magnetron Facility (RF Priming).

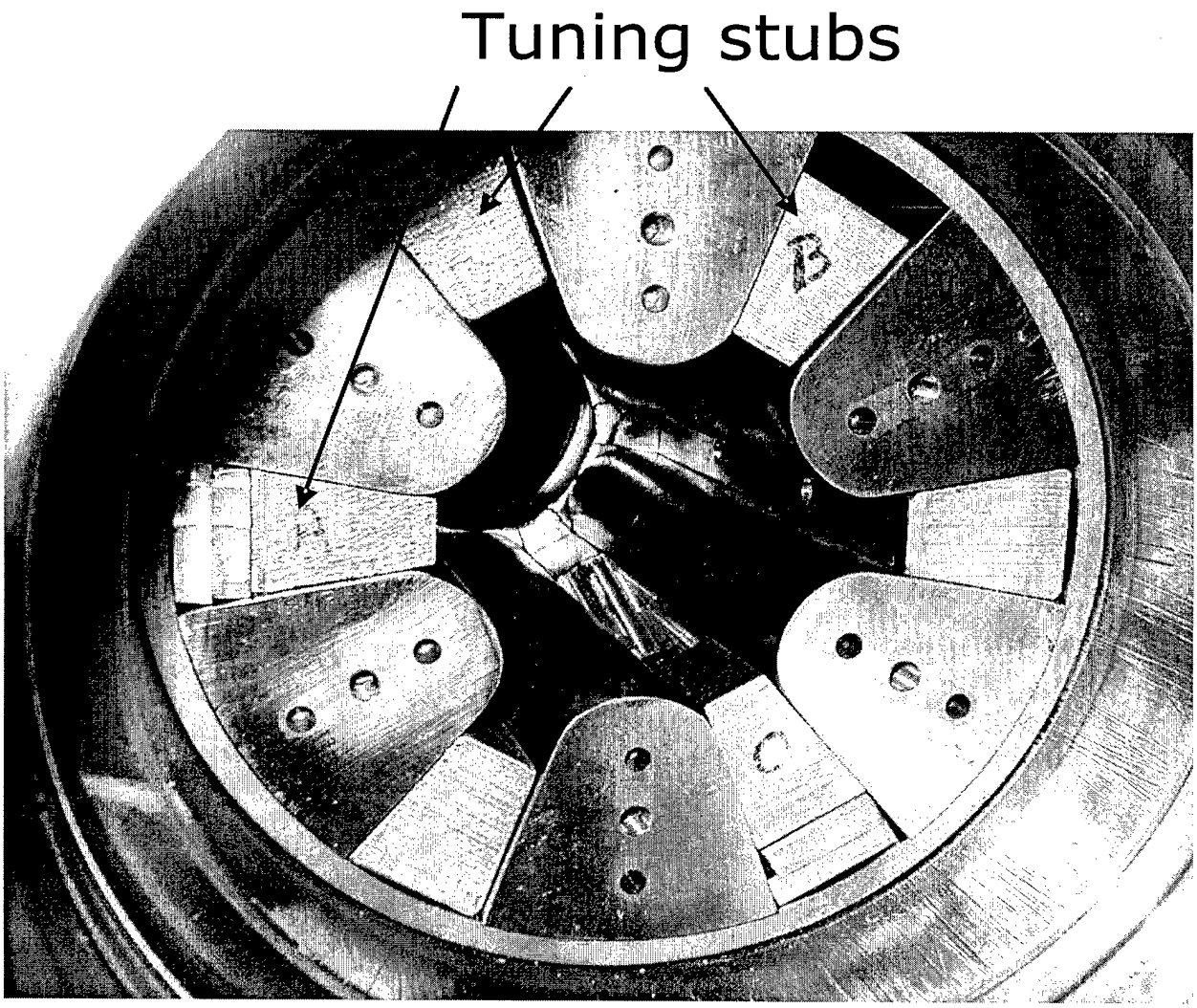

Figure 3: Photograph of magnetron anode block with tuning stubs.

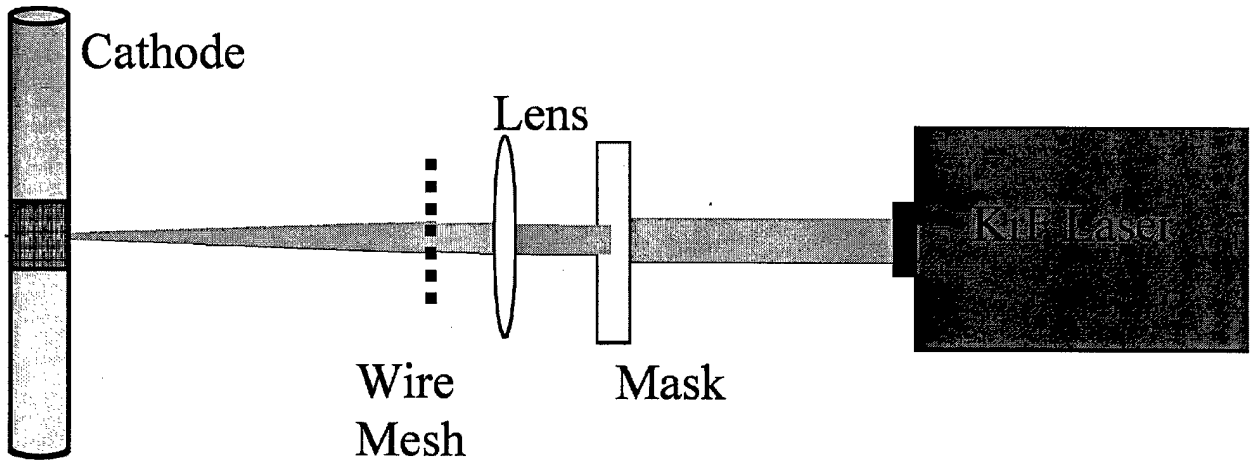

Figure 4. Projection Ablation Lithography (PAL) Cathode fabrication experimental configuration.

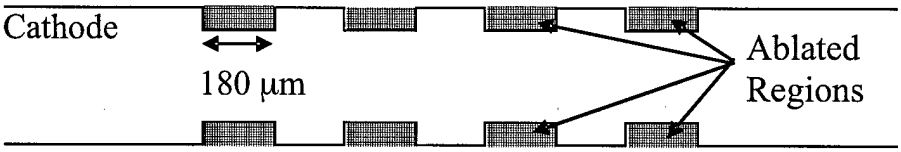

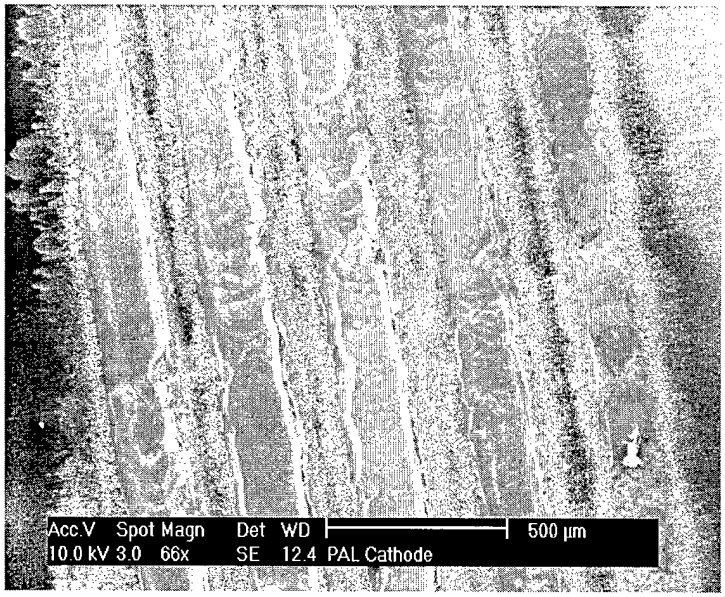

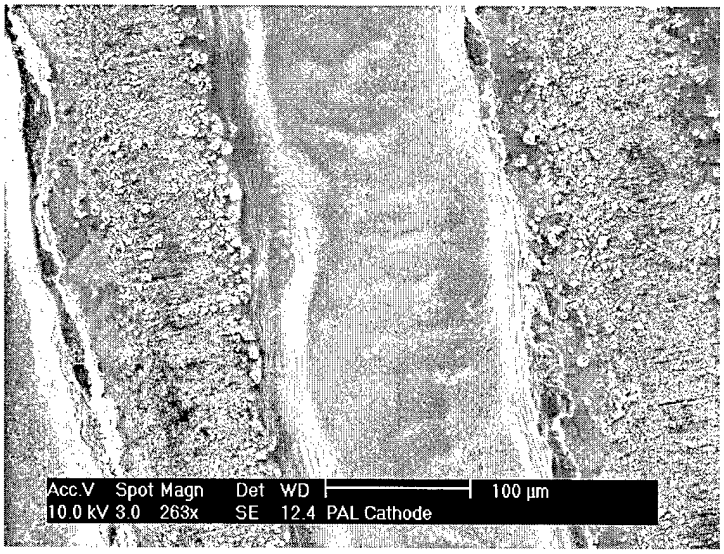

Figure 5. a) Schematic depiction of PAL laser ablation design. b,c) Scanning Electron Microscope photos of PAL cathode.

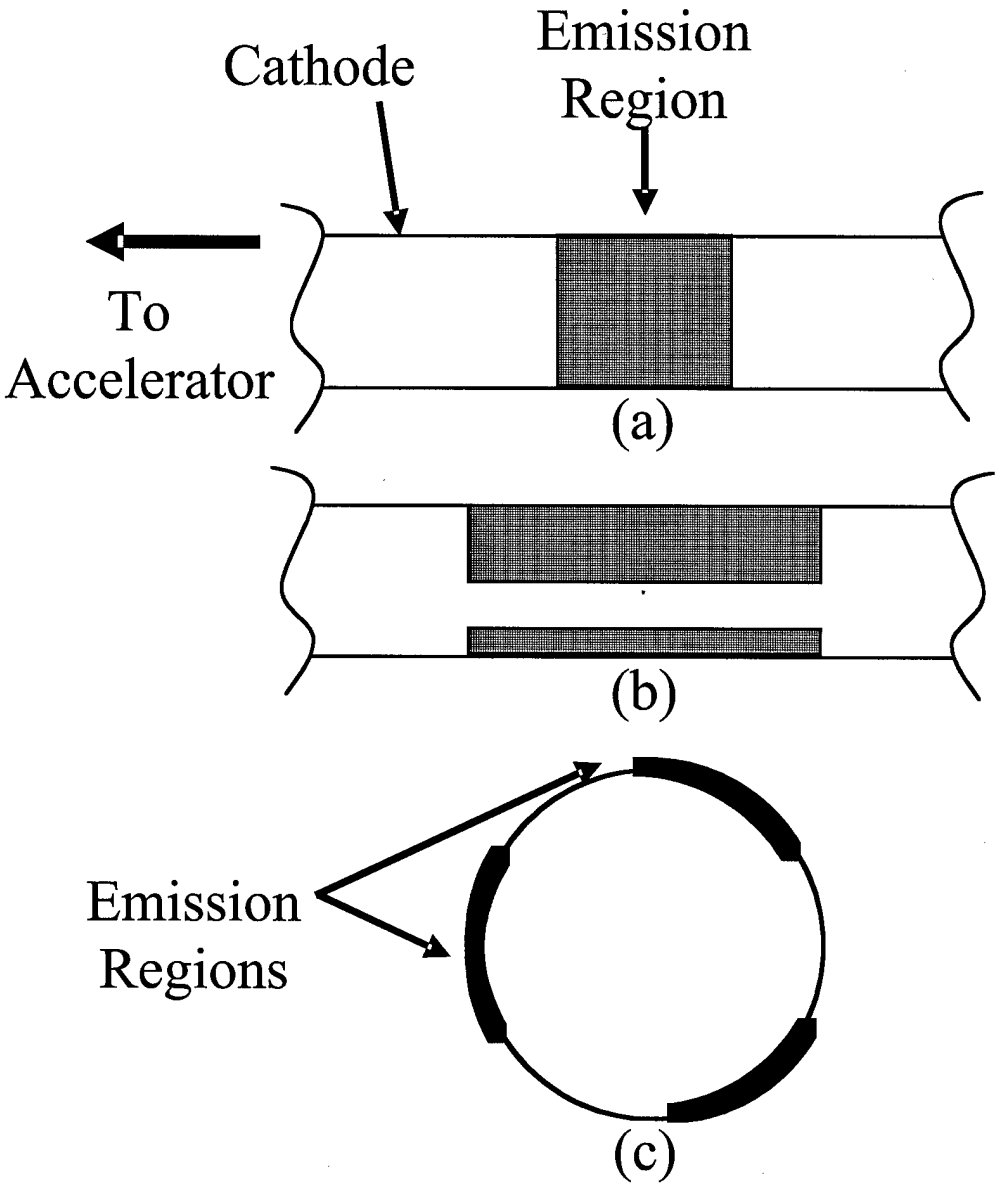

Figure 6. Configuration of Tri-PAL cathode for cathode priming.

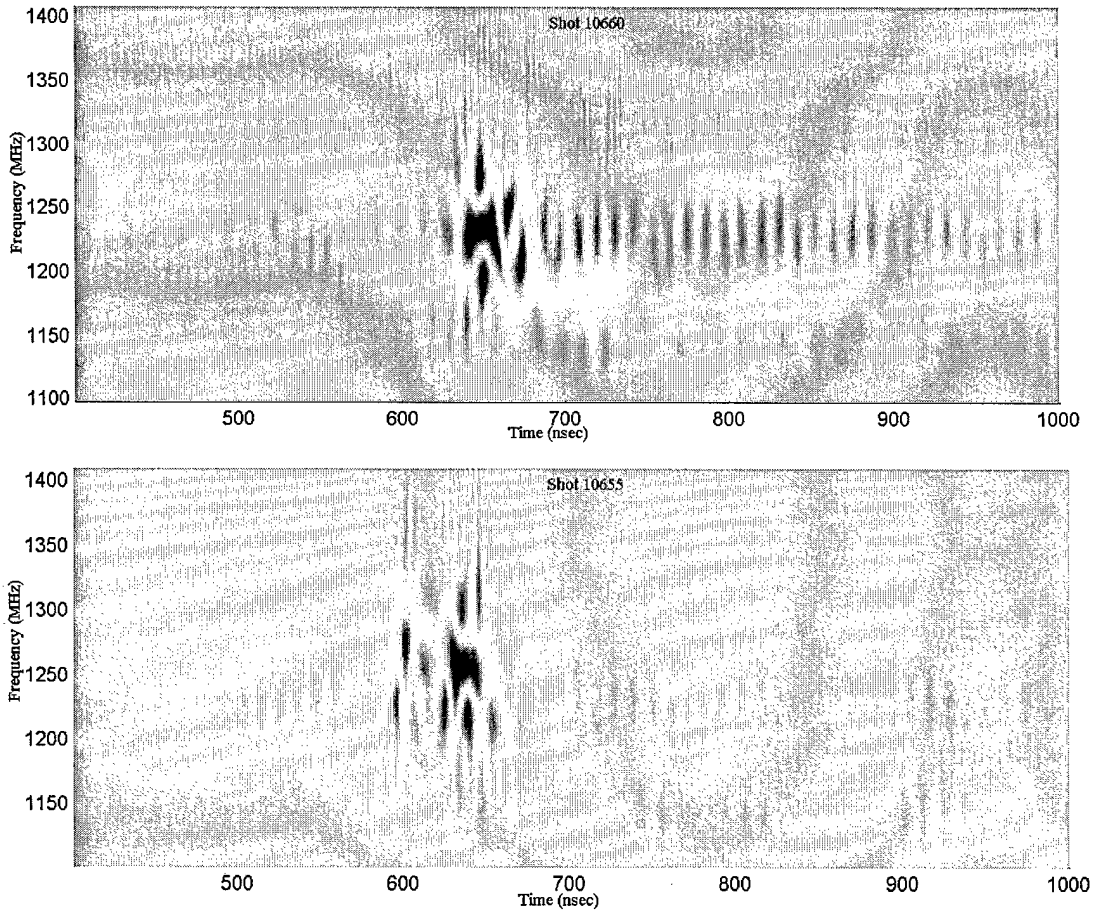

Figure 7. Two representative TFA (time-frequency-analysis) data sets for primed relmag shots. Note that in the lower shot the relmag is operating at the primed frequency (1.28 GHz) for the 2*pi/3 mode.

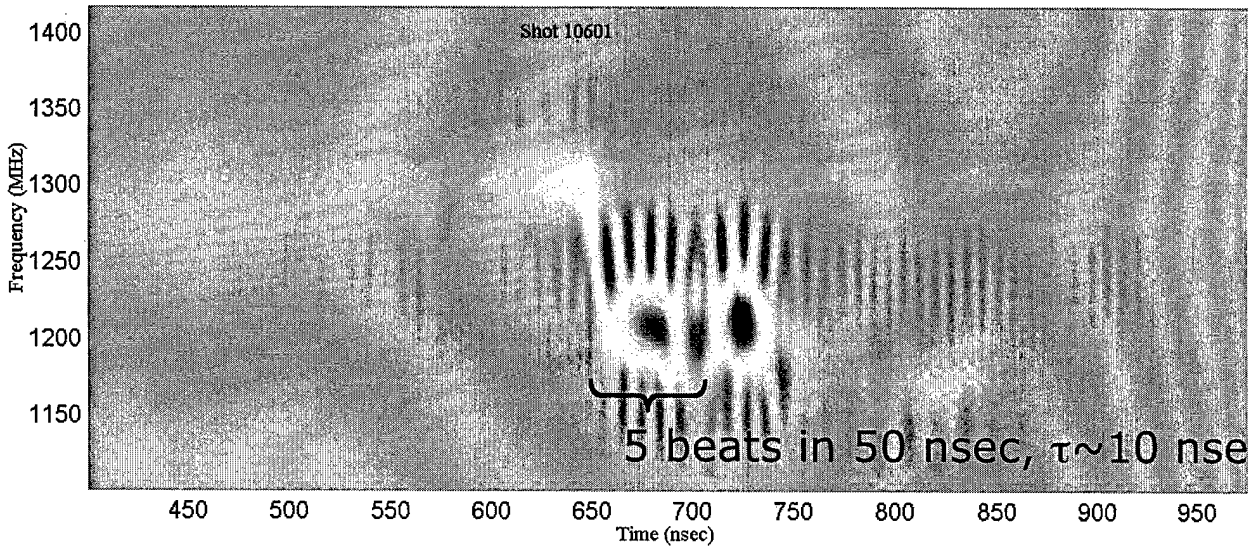

Figure 8. TFA data displaying the characteristic "mode beating" for priming magnetron detuned slightly from relativistic magnetron 2*pi/3 mode.

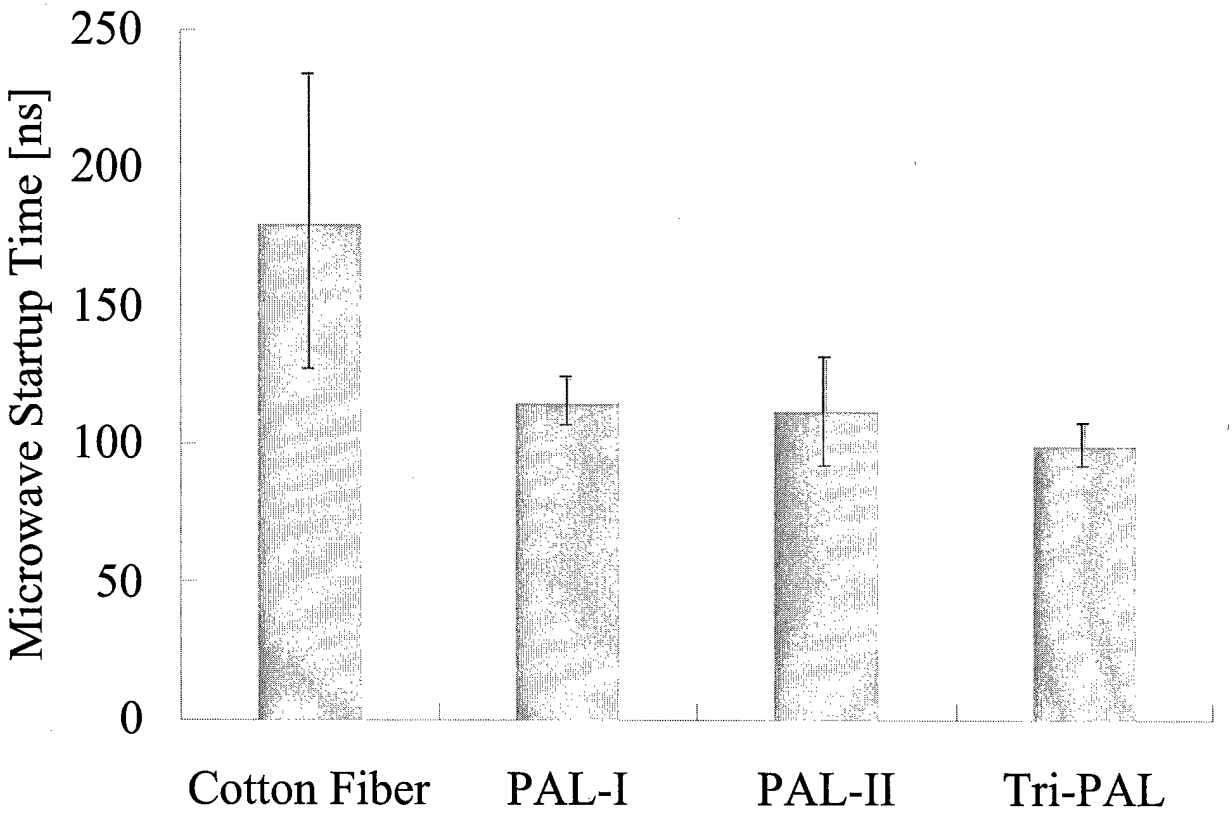

Figure 9. Summary and comparison of start-oscillation times for cathode priming (Tri-PAL) cathode versus single emission zone cathodes.

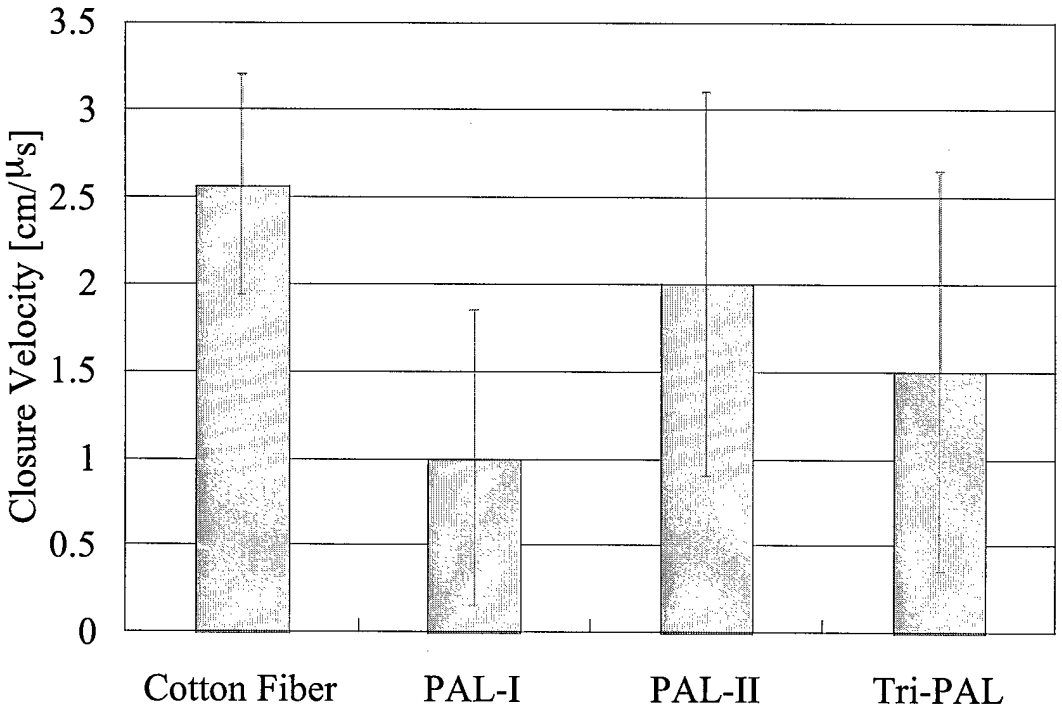

Figure 10. Summary data of plasma closure velocities for PAL cathodes compared to previous cotton cathode.

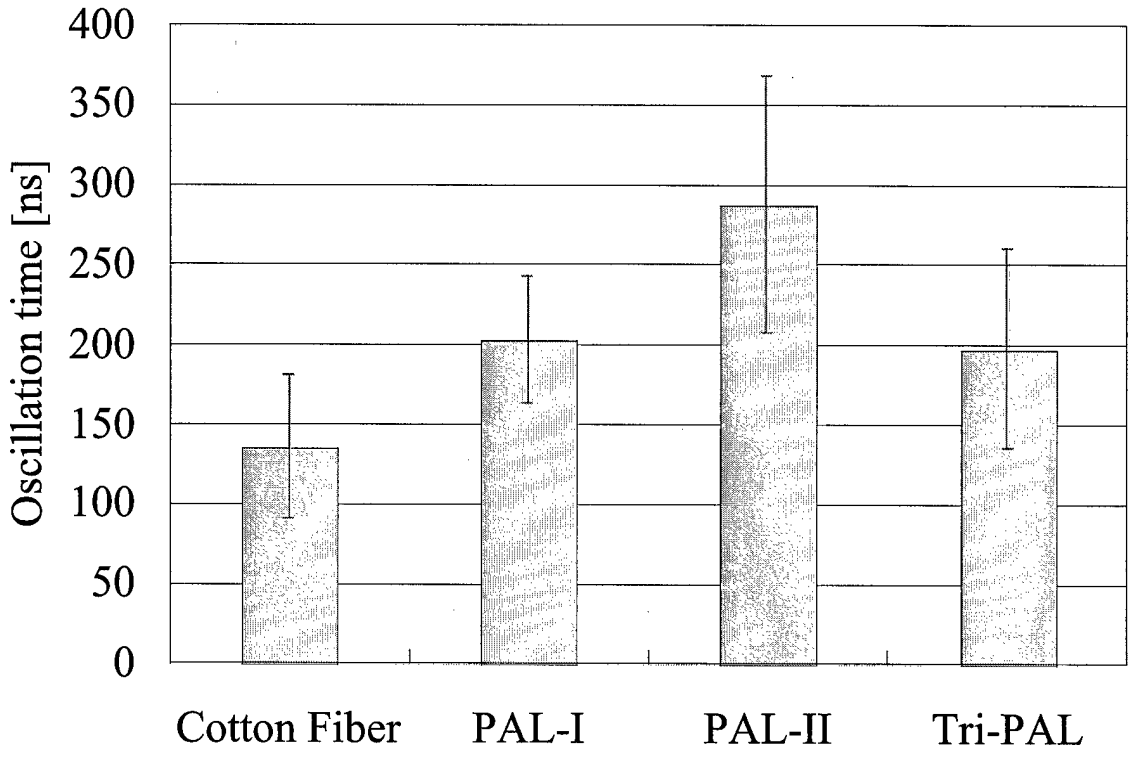

Figure 11. Summary and comparison of microwave pulselength for PAL cathodes versus cotton cathode.

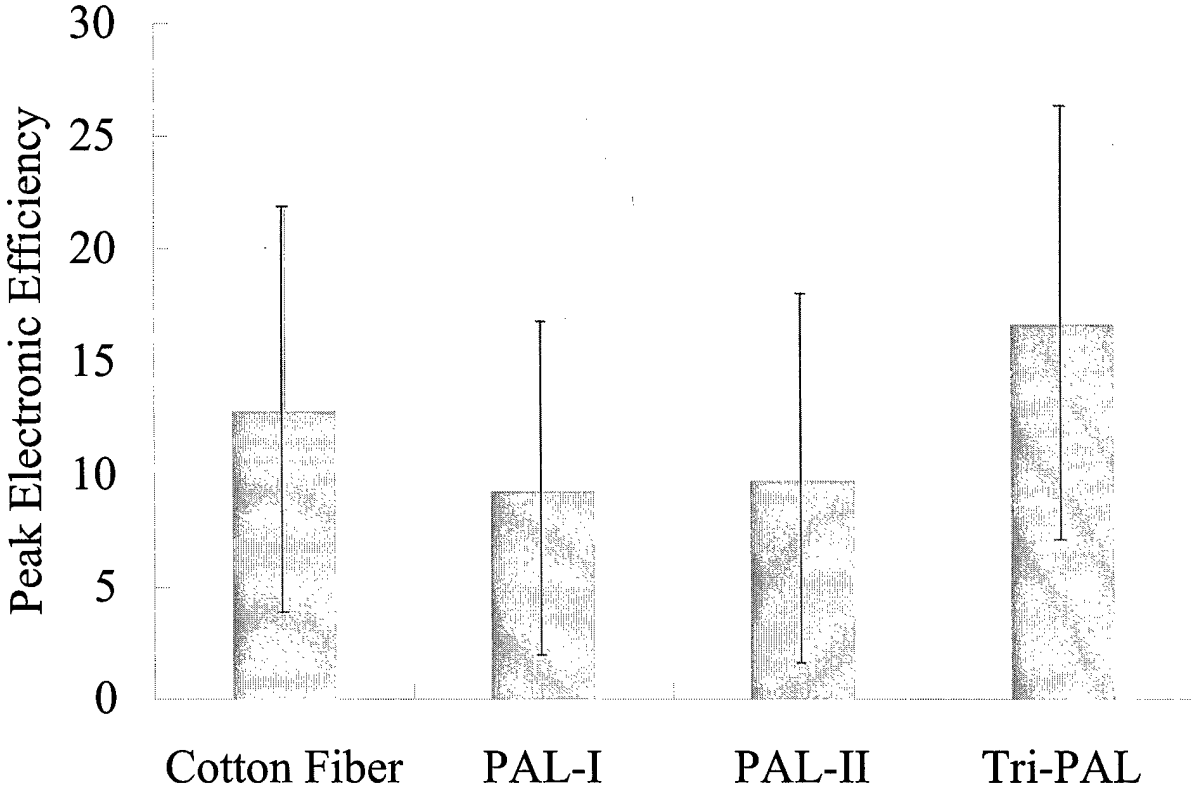

Figure 12. Peak electronic efficiency of microwave generation in the relativistic magnetron for PAL cathodes compared to the cotton cathode.

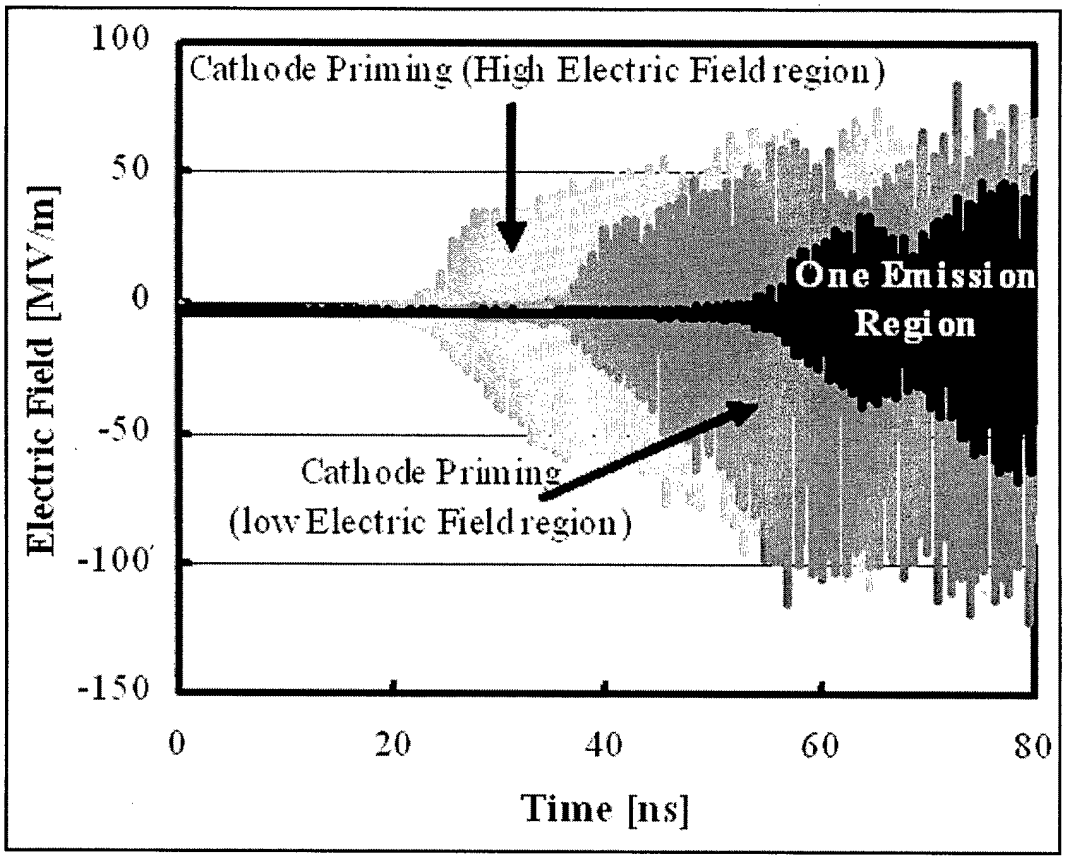

Figure 13: 2D MAGIC Code Simulation of cathode priming versus single emission region. Two orientations of emitting strips are shown: high electric field (under vanes) and low electric field (under cavities).

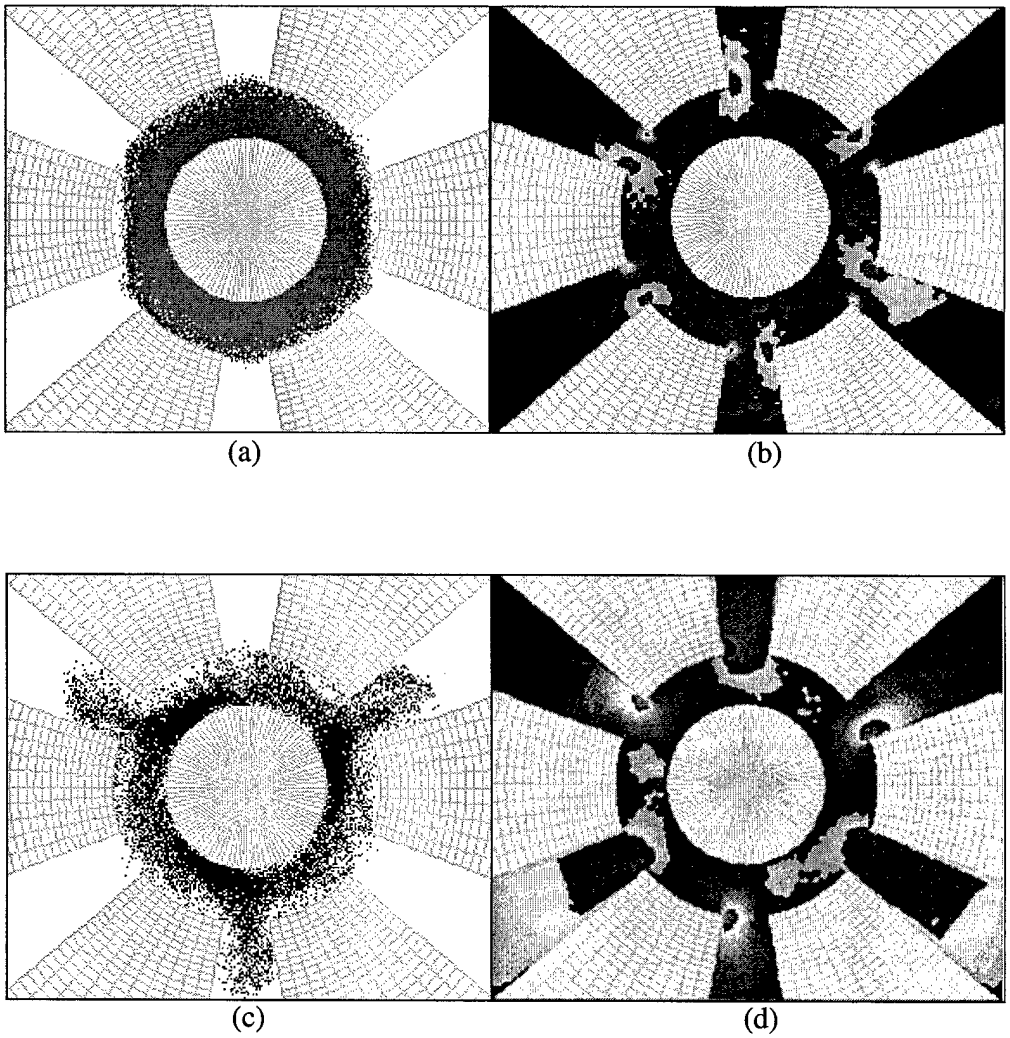

Figure 14: Electron phase-space plots and RF fields at 3-D MAGIC Code simulation time of 6.5 ns for (a), (b) no priming versus (c), (d) cathode priming with emission centered under the anode vanes.

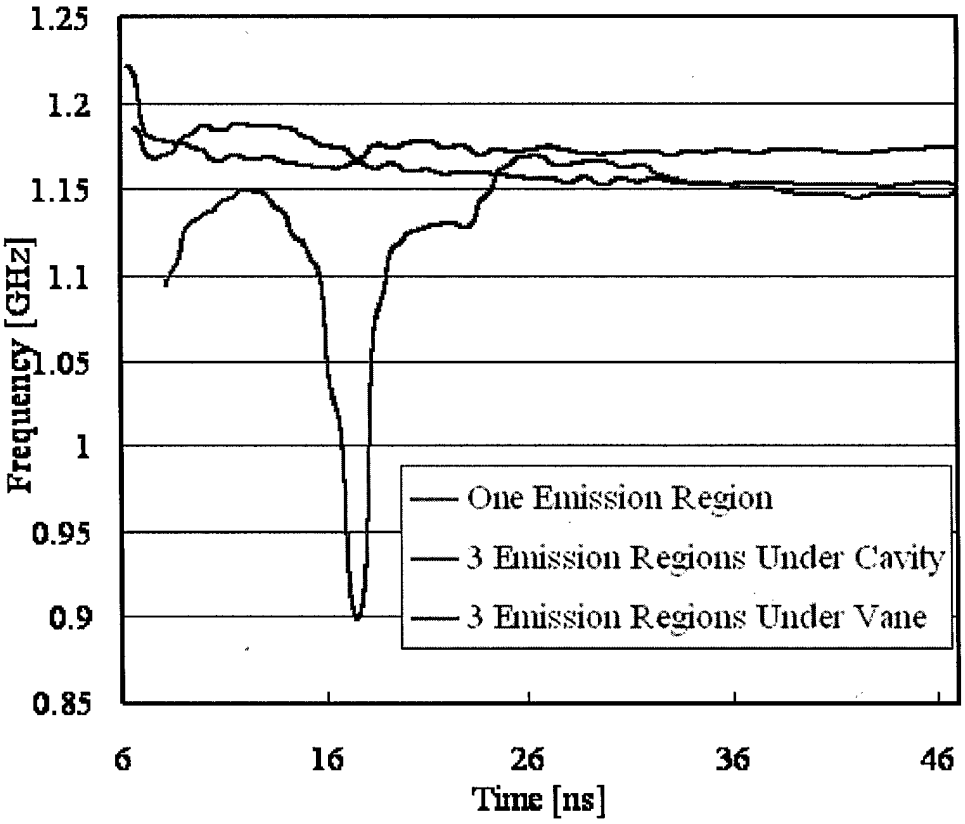

Figure 15. Instantaneous frequency of the A6 relativistic magnetron with cathode priming versus single emission region cathode.(3D MAGIC Code simulation).

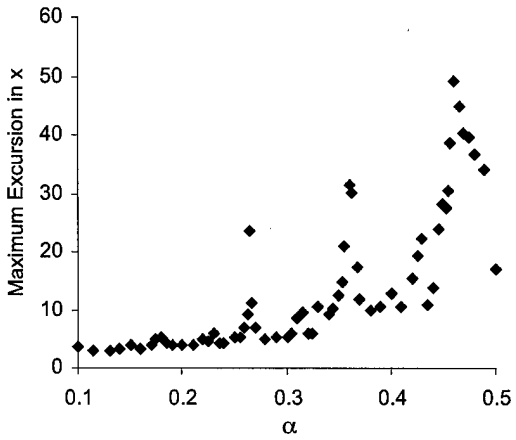

Figure 16. Electron maximum excursion as a function of α, the magnetic priming strength. The electron maximum excursion peaks in certain bands of α

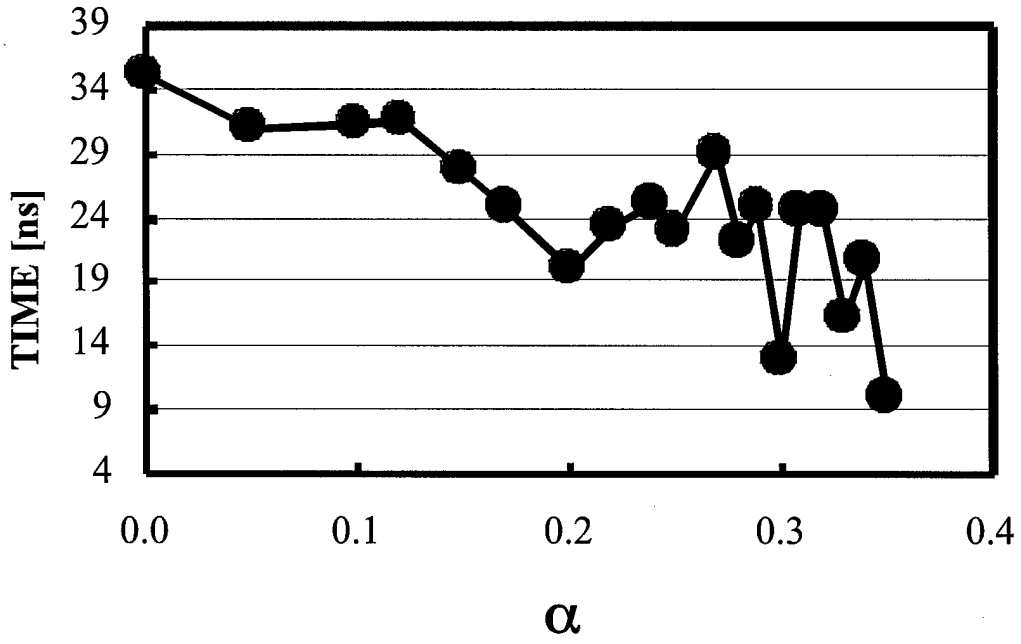

Fig.17. Startup time for the pi-mode versus magnetic priming strength, α, according to MAGIC simulations of the Titan/UMich relativistic magnetron. Certain values of α yield shortest startup time, indicative of some resonant (parametric?) process.

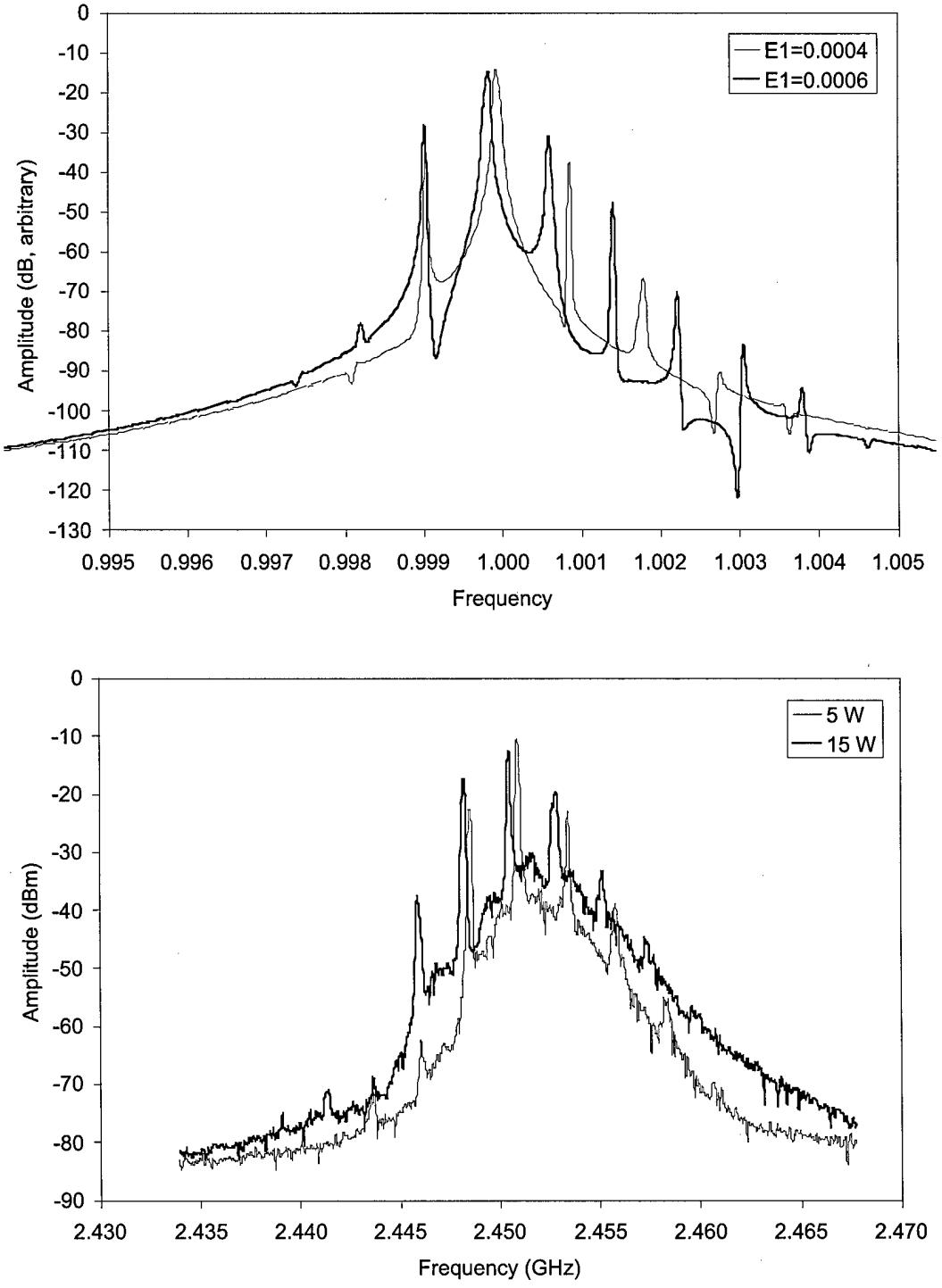

Figure 18. Reflection amplifier microwave spectra: 1. (top) theoretical model, 2. (bottom) experimental data when P_{drive} are 5 and 15 W.

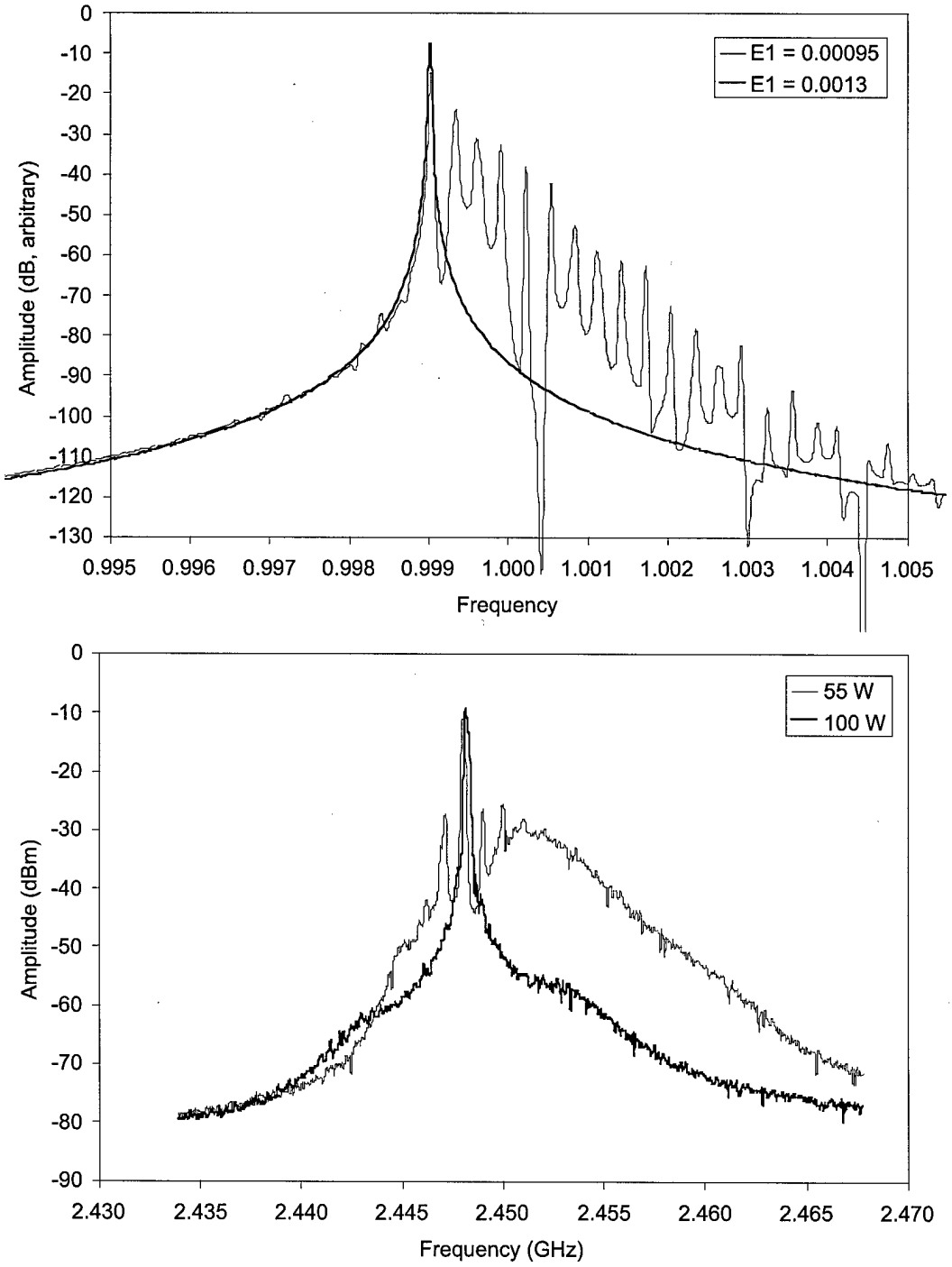

Figure 19. Reflection amplifier microwave spectra: 1. (top) theoretical model, 2. (bottom) experimental data when P_{drive} are 55